Article citation info:
DASZKIEWICZ, P., ANDRZEJEWSKI, M., MEDWID, M. et al. Analysis of the selection of chosen technical parameters of the power-train system for a diesel-electric rail-road tractor. *Combustion Engines*. 2021, **186**(3), 64-71. https://doi.org/10.19206/CE-140723

Paweł DASZKIEWICZ
Maciej ANDRZEJEWSKI
Marian MEDWID
Patryk URBAŃSKI
Maksymilian CIERNIEWSKI
Aleksandra WOCH
Natalia STEFAŃSKA

Combustion Engines
Polish Scientific Society of Combustion Engines

Analysis of the selection of chosen technical parameters of the powertrain system for a diesel-electric rail-road tractor

ARTICLE INFO

Received: 7 July 2021
Revised: 30 July 2021
Accepted: 1 August 2021
Available online: 8 August 2021

The article presents the results of a simplified analysis of the feasibility of designing a rail chassis of a two-way tractor with an internal combustion or electric drive. Basic traction and operating parameters have been assumed for which the road-rail tractor could operate in an effective manner. On their basis, strength calculations were carried out and mechanical elements of the drive system meeting the required assumptions were selected. All the calculations presented in the text were fulfilled. The technical feasibility of building the mechanical part of the rail running gear of a rail-road tractor driven by an internal combustion engine or electric motors has been demonstrated.

Key words: *rail-road tractor, electric drivetrain, zero emission, rail chassis, diesel-electric vehicle*

1. Introduction

The increasingly restrictive exhaust emission norms [9] force vehicle manufacturers to reduce the exhaust emissions [51, 52] and the fuel consumption [38] of their products. This also applies to manufacturers of rolling stock [45] where, in order to be permitted into operation, rail vehicles equipped with internal combustion engines must be equipped with environmentally friendly high-efficiency combustion engines [47] and exhaust aftertreatment systems [1, 8]. These solutions focus mainly on the modernization of vehicles [34], the use of batteries [21], including the most cutting-edge ones, such as Na-Ion [44], and adding ultracapacitors [46] to rail vehicles, hybridization [2], the use of alternative fuels [37, 39] and using various types of fuel cells [10]. The driving style can also significantly affect the resulting exhaust emission indicators [1]. However, the significant age of the rolling stock operated nationally results in increased exhaust emissions, especially during shunting works where the engine operating conditions are transient and changing [15].

This reason was the driving force behind the development of new shunting solutions in which for this type of work requiring significant power output [41] values, agricultural tractors, adapted to moving along the tracks and powered by a smaller combustion engine, were used instead of the conventional solutions [28, 30]. The main advantage of such solutions comes from their affordability, where the tractor is several times cheaper to purchase and operate than an average shunting locomotive. The use of this type of vehicle drive, despite its much lower emissions compared to diesel locomotives, still exposes the environment to the effects of harmful exhaust compounds [11, 33], especially when the vehicles are operated in enclosed spaces, such as in construction halls where air circulation is limited. Hence people remaining in the vicinity of a running vehicle are exposed to the effects of toxic exhaust gas compounds [40].

There are solutions using hybrid [36] and electric [5, 32] agricultural tractors as well as tractors used in greenhouses [22] around the world. Projects aimed at electrification of the agriculture sector were implemented, including innovative ones, such as an electric tractor powered through cables [43]. There have also been concepts of tractors that would use alternative energy sources such as solar energy [48]. Vehicles of this type require many complex and innovative technical solutions, such as in case of the suspension system [12], the fuel supply system [13], the steering system [19], and energy management [23, 24, 35, 42]. Analyzes of the economic feasibility of implementing an electric drive system for Diesel tractors [16], traction tests [25] and battery behavior tests [7] are also carried out. Works related to the widespread use of tractors with alternative drive are at a very advanced stage, especially in China [4], where increasing productivity in agriculture remains possible thanks to automation, robotization and the breeding of new, more durable varieties of plants [20]. These solutions, however, make it impossible to adapt vehicles to run on rails due to design factors.

The paper [27] presents the design expectations and the conceptual model of a rail-road tractor with a diesel-electric drive, where design solutions for the rail undercarriage rollers drive and braking were presented, which at the same time also had to meet all the legal requirements [6].

The next stage of the assessment of project feasibility and compliance with the outlined design parameters involved analyzes and simulations of the selection of basic parameters, such as electric motor power, energy storage capacity and several other mechanical parameters of the drive system [31] and tractor braking.

2. Project description

The diesel-electric tractor was designed on the basis of rail-road diesel tractors designed in Łukasiewicz – IPS „TABOR" [3, 26, 29]. The main structural elements with

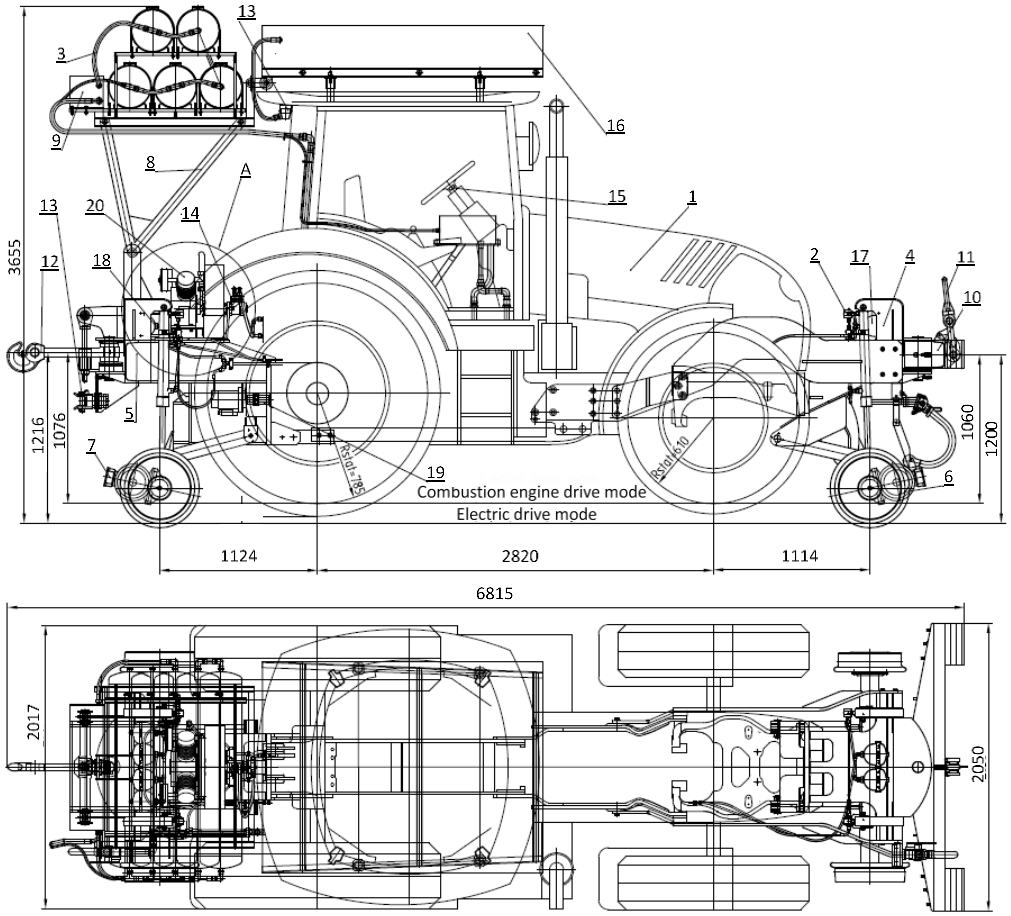

Fig. 1. Tractor concept model based on Arion-610: (1) combustion engine cover, (2) the system of hydraulic pressure on the rollers to the track, (3) pneumatic system of the railway brake, (4) front pull-buffer mechanism, (5) rear pull-buffer mechanism, (6) front running gear with electric drive, (7) rear running gear with electric drive, (8) mounting frame for the air tanks, (9) pneumatic control panel, (10) front buffer beam, (11) front coupler, (12) rear coupling hook, (13) electrical installation, (14) compressor drive (hydraulic or electric), (15) steering wheel lock, (16) energy storage devices, (17) hydraulic accumulators of the front rollers, (18) hydraulic accumulators for rear rollers and compressors, (19) alternator driven from the PTO shaft, (20) compressor for railway brake

which the tractor was additionally equipped, based on the calculations, were: electric motors, reduction gears, electromagnetic clutches, a battery set and an alternator [50] as a source of drive for the guide rollers of the rail running gear. The tractor concept has been shown in Fig. 1.

The basic mode of tractor operation is work in open terrain powered by the combustion engine. The tractor can be powered by an electric motor e.g. when rolling the towed rolling stock into and out of inspection halls and during maneuvers in enclosed spaces.

In the electric driving mode, the main source of drive torque are the guide rollers of the rail drive chassis, which are driven by electric motors installed on the rail axles at both guide rollers or by one motor driving both guide rollers. The entire weight of the tractor in such situation rests on the guide rollers. Tractor tires are raised so that they make no contact with the ground.

The assumed geometrical parameters of the drive system (diameter of the internal gear of the roller and the diameter of the motor gear) allow to obtain the maximum gear ratio i_{z1} = 8.6, with a diameter of the guide roller of 500 mm. A two-stage reduction gear with a planned gear ratio of i_{zp} = 49 was connected to each of the guide roller sets to enable the use of conventional electric motors, which are to operate under optimal parameters (rotational speed and load) [18]. This solution was also chosen as a method of eliminating high-power electric motors which are greater in size, weight, energy consumption and cost. When driving in electric mode during shunting work, the guide rollers rotate at a low speed that requires a significant amount of torque and results in low travel speeds. For this reason, failure to use the reduction gear would result in inefficient operation of the electric motors at low rotational speeds, which would translate into significant energy losses. It should also be remembered that driving on rails at higher speeds in combustion engine mode requires the use of guide rollers that are mechanically connected to electric motors. Higher cruising speed and the use of reduction gears would drive the electric motor shaft to significant rotational speed values, and thus would significantly load the electric motor bearings. Such a phenomenon can significantly increase the probability of motor failure. For this reason an electromagnetic clutch is to be included in the drive system, which is expected to increase its overall reliability.

3. Analysis of the selection of drive system parameters

3.1. Electric motor dimensions

Variant I. The electric drive of the guide rollers shown in Fig. 2 consists of: an asynchronous electric motor (1) with low rotational speed, an electromagnetic clutch (2), an internal gear (3), a wheel (4) and bearings (5, 6). Each of the four guide rollers of the rail-road tractor consists of such a set of devices. The electric motor is additionally equipped with an electromagnetic parking disc brake, built inside, in the rear portion of the vehicle. The electric motor is connected to the internal gear installed in the guide roller wheel through an electromagnetic clutch. The electromagnetic clutch disengages the electric motor from the roller only when the roller is not used to drive the vehicle, i.e. it acts as a guide on the track (when the tractor operates using the diesel drive).

The guide roller in the diesel-electric tractor has an increased rolling diameter from ϕ400 mm to ϕ500 mm. This is in order to make enough room to install an internal gear (with a specific ratio), an electric motor (large dimensions) as well as due to an increased load on the guide roller. Due to their considerable size, the two electric motors driving two rollers on the same axis must be shifted to positioned at an angle of approx. 90° to each other.

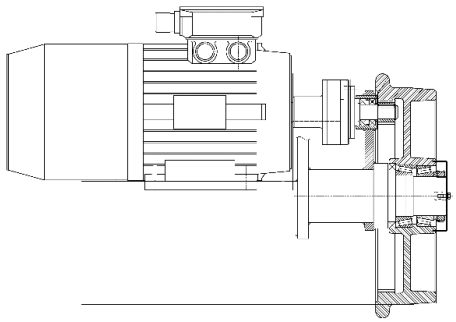

Fig. 2. Electric drive of a guide roller with a 5kW motor and 720 rpm

Variant II. The guide roller electric drive shown in Fig. 3 has an inbuilt asynchronous electric motor with a higher nominal rpm value. The exploitation of higher drive speed increases the power requirement for the same torque. In this solution, it would be advisable to electrically limit the high rotational speed of the drive motor. Two motors driving two guide rollers on the same axis are compact enough to be mounted in the same plane.

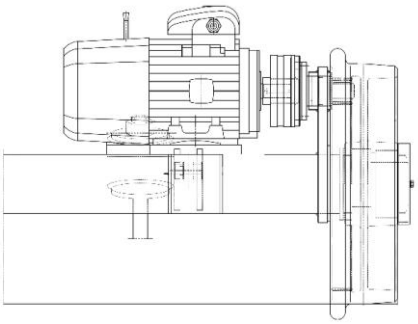

Fig. 3. Electric drive of a guide roller with a 5 kW motor and 1430 rpm

Variant III. The guide roller electric drive (variant III) shown in Fig. 4 has a built-in MeMax 1718 – Sin/Cos, BLDC brushless permanent magnet synchronous electric motor. Such a solution of the electric drive, due to the small longitudinal dimensions of the motor, enables optimal use of parameters and makes it possible to mount two motors on one axis. Table 1 presents the parameters of three variants of electric motors that could be installed on a rail-road vehicle.

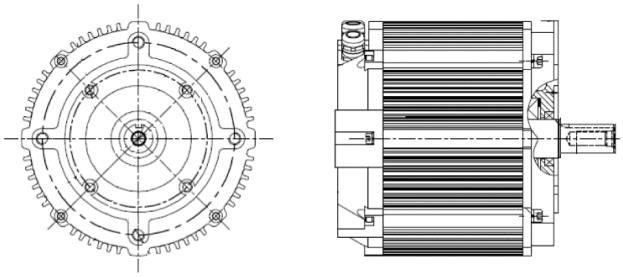

Fig. 4. BLDC electric motor for drive of a guide roller with a 6 kW and 3200 rpm

Table 1. Electric motors operating parameters

Parameter	Variant		
Number [–]	I	II	III
Power [kW]	5.5	5	6
Max motor speed [rpm]	720	1445	5500
Rated current [A]	15.3 (400 V)	15.3 (400 V)	125 (48 V)
Max. torque [Nm]	73	71.1	39
Nominal torque [Nm]	25.2	33	14.3
M coefficient (M_{max}/M_{nom}) [–]	2.9	2.2	2.7
Mass [kg]	84	35	13.8

The analysis of the motor dimensions (Fig. 2) shows that the installation of two motors on the rail axis in one plane is not possible due to the limited length of the rail axis. However, two motors can be installed at an angle of 90° relative to each other. Such a solution was rejected due to the lack of symmetry of the electric motor installation, although technically such a solution is possible in the project implementation.

Figure 3 shows the mounting of a 5 kW motor with a speed of 1430 rpm. A motor with smaller dimensions compared to variant I meets the size conditions, but due to its considerable weight and larger longitudinal dimensions compared to variant III, it would not be optimally used in such a configuration.

The mounting conditions and assumed operating parameters of the tractor are met by the BLDC motor with a nominal power of 6 kW, which was shown in Fig. 4. This solution of the vehicle guide roller drive enables the optimal use of the motor operating parameters and the optimal fit of the two motors on one rail axis. Significant advantages of the motor used are its small longitudinal dimensions and low weight, while maintaining favorable traction parameters.

3.2. Vehicle drive technical parameters

The elements of the electric drive module for the diesel rail-road vehicle were selected based on the following calculations and assumptions under which the vehicle was to

operate. The main assumption was the prerequisites for starting (Table 2).

Table 2. Electric module drivetrain operating parameters

Parameter	Value	Unit
Acceleration – a	0.05	[m/s^2]
Startup time – t	3	[s]
Wheel diameter	0.5	[m]
1st stage gear ratio – i_{z1}	8.6	[–]
2nd stage gear ratio – i_{zp}	25	[–]
Total gear ratio – i_c	215	[–]

Then the initial speed of the vehicle would equal:

$$V = a \cdot t = 0.05 \cdot 3 = 0.15 \text{ m/s} = 0.54 \text{ km/h} \quad (1)$$

and the rotational speed n_k of the guiding roller would be:

$$n_k = \frac{60 \cdot V}{\Pi \cdot D_k} = \frac{60 \cdot 0.15}{3.14 \cdot 0.5} = 5.7 \text{ rpm} \quad (2)$$

the electric motor rotational speed n_s:

$$n_s = n_k \cdot i_c = 5.7 \cdot 215 = 1232 \text{ rpm} \quad (3)$$

The following assumptions were made for further calculations:

– mass of 4 empty wagons: $m_w = 4 \cdot 30 = 120$ Mg
– mass of the diesel-electric tractor: $m_c = 10.5$ Mg.

The force of inertia of the towed rail set P_b at the moment when movement begins becomes:

$$P_b = (m_t + m_w) \cdot a = (120 + 10.5) \cdot 0.05 = \\ = 6.525 \text{ Mg} = 6525 \text{ N} \quad (4)$$

Thus, for a single wheel:

$$P_{b1} = 6525 : 4 = 1631 \text{ N} \quad (5)$$

Guide roller wheel driving torque M_{ok}:

$$M_{ok} = \frac{P_1 \cdot D_k}{2} = \frac{1631 \cdot 0.5}{2} = 408 \text{ Nm} \quad (6)$$

Electric motor torque [50]:

$$M_{os} = \frac{M_{ok}}{i_c} = \frac{408}{215} = 1.9 \text{ Nm} \quad (7)$$

Maximum power demand of the electric motor $N_{S\,max}$:

$$N_{Smax} = \frac{M_{Os} \cdot n_{Smax}}{9550} \quad (8)$$

where: $n_{s\,max}$ =5500 rpm – max electric motor rotational speed, n_s = 1232 rpm – electric motor speed when beginning to move.

Hence:

$$N_{Smax} = \frac{M_{Os} \cdot n_{Smax}}{9550} = \frac{1.9 \cdot 5500}{9550} = 1.09 \text{ kW} \quad (9)$$

The electric motor has a significant power demand (max. 12 kW for this motor type) at maximum rotational speeds, so the vehicle should be started at a lower motor speed, regulated with the BLDC motor by changing the voltage supplied [17].

Then:

$$N_S = \frac{M_{Os} \cdot n_S}{9550} = \frac{1.9 \cdot 1231.9}{9550} = 0.245 \text{ kW} \quad (10)$$

The rotational speed of the electric motor while starting the vehicle should amount to n_s = 1200 rpm. Starting and braking with the vehicle while under loaded should take place at speeds not exceeding $V_r \approx 0.5$ km/h, i.e. up to the rotational speed of electric motors $n_r \approx 1150$ rpm. While driving, the rotational speed of the motors should be changed electrically depending on what is necessary, up to the value of $n_{max} \approx 5500$ rpm, thus obtaining the vehicle maximum cruising speed of: $V_{max} \approx 2.5$ km/h.

3.3. The gear transmission selection

Earlier, in the calculations of the torque values, the gear ratio i_z = 8.6 was assumed as the result of mounting the electric motors on the axle inside the rail wheel assembly. The smallest wheel diameter was chosen based on the limited number of teeth resulting from undercutting the contour during the cooperation of the wheels. $z_1 = z_g = 17$ teeth for the values $\alpha_0 = 20°$ and y = 1 as well as the number of teeth z_2:

$$z_2 = z_1 \cdot i_z = 17 \cdot 8.6 = 146 \quad (11)$$

Gear teeth module m_0:

$$m_0 = 2.71 \cdot \sqrt[3]{\frac{M_0}{\psi \cdot \lambda \cdot z \cdot k_{go}}} \text{ mm} = \\ = 2.71 \cdot \sqrt[3]{\frac{47400}{13 \cdot 3.26 \cdot 17 \cdot 40}} = \\ = 2.71 \cdot 1.18 = 1.5 \text{ mm} \quad (12)$$

where: precise execution with one-sided bearing (wheel sagging):

$$\Psi_{max} = \frac{b_S}{m_o} = \frac{40}{3} \approx 13 \quad (13)$$

– for the wheel with a zero contour displacement $\lambda = 3.26$,
– for 10^5 load cycles:

$$k_{go} = 0.38 \cdot R_m \cdot C_c = 0.38 \cdot 550 \cdot 2 = \\ = 420 \text{ MN/m}^2 = 42 \text{ N/mm}^2 \quad (14)$$

– $C_c = 2$ and when the wheel is made of steel casting (R_m = 550 M_n/m^2), M_0 = 47.4 Nm = 47400 Nmm.

The gear teeth modulus m_0 = 3 mm was used, assuming better material for the wheels and improving the mounting of the small wheel (introducing bearings). Also greater loads are foreseen for the toothed wheel.

The diameters of the gears D_1 and D_2 are:

$$D_1 = z_1 \cdot m_0 = 17 \cdot 3 = 51 \text{ mm} \quad (15)$$

$$D_2 = z_2 \cdot m_0 = 146 \cdot 3 = 438 \text{ mm} \quad (16)$$

3.4. Electromagnetic clutch selection

The fundamental parameter used to guide the selection of the electromagnetic clutch is the torque on the shaft between the two-stage gearbox and the internal gear, which equals M_{os} = 47.4 Nm. Hence, the EZM1-80-5-24 type

clutch was chosen with technical parameters as presented in Table 3. The nominal torque of the clutch is many times greater than the torque transmitted by the electric motor.

Table 3. Technical parameters of the selected electromagnetic clutch

Parameter	Value	Unit
Clutch size	80	[–]
Nominal torque	1000	[Nm]
Coil power	40	[W]
Max motor speed	2500	[rpm]
Operation	dry	[–]

4. Checking the guide roller bearings

The following sizes of SKF tapered roller bearings are used in existing track rollers on rail-road tractors:

– no. 33019 dimensions ϕ95/145×39 and a load capacity of C = 15000 daN
– no. 33018 dimensions ϕ90/140×39 and a load capacity of C = 14300 daN.

The equivalent force P_z acting on the bearings is calculated as follows:

$$P_z = X\,F_r + Y\,F_a = 1 \cdot 3000 + 0 \cdot 262.5 = 3000 \text{ daN} \quad (17)$$

where: maximum radial force F_r acting on the roller wheel with the tractor lifted: F_r = 30 kN = 3000 daN, longitudinal force on the wheel F_a:

$$F_a = F_{r\,tg\alpha} = 3000 \cdot tg50 = 262.5 \text{ daN} \quad (18)$$

the following indicators were taken from the bearing catalog:

$$e = \frac{F_a}{F_r} = \frac{262.5}{3000} = 0.087 \quad (19)$$

for e < 0.27 and Fa/C = 0.0175 these values are X = 1, Y = 0.

The bearings dynamic load capacity $C_{calc.}$ was verified using the following formula:

$$C_{calc.} = \frac{f_h \cdot P_z}{f_n \cdot f_t} \text{ daN} \quad (20)$$

where: temperature factor: f_t = 0.9 for t > 200°C, operating time: L_h = 10000 h, bearings rotational speed: n_{min} = 5.7 rpm and n_{max} = 220 rpm.

Hence the operating time factor is:

$$f_h = \sqrt[3.33]{\frac{L_h}{500}} = \sqrt[3.33]{\frac{10000}{500}} = \sqrt[3.33]{20} = 2.459 \quad (21)$$

And the rotational speed factor f_n is [14]:

$$f_{n\,min} = \sqrt[3.33]{\frac{33.3}{n_{min}}} = \sqrt[3.33]{\frac{33.3}{5.7}} = \sqrt[3.33]{5.84} = 1.699 \quad (22)$$

$$f_{n\,max} = \sqrt[3.33]{\frac{33.3}{n_{max}}} = \sqrt[3.33]{\frac{33.3}{220}} = \sqrt[3.33]{0.1514} = 0.567 \quad (23)$$

Hence the calculated dynamic load capacities of the bearings are:

$$C_{calc.min} = \frac{2.459 \cdot 3000}{1.699 \cdot 0.9} = 4824 \text{ daN} \quad (24)$$

$$C_{calc.max} = \frac{2.459 \cdot 3000}{0.567 \cdot 0.9} = 14448.3 \text{ daN} \quad (25)$$

and the total dynamic load capacity of the bearings becomes:

$$\Sigma C = 15000 + 14300 = 29300 \text{ daN} > C_{calc.} \quad (26)$$

5. Air brake selection for the rail drive

The block brake is installed in the outer cavity of the guide roller (Fig. 5) for the four guide rollers of the rail undercarriage. The friction brake is designed to brake only the weight of the tractor itself. Braking of a tractor with wagons train set is performed with the use of a pneumatic railway brake supplied with air from a compressor installed in the rear part of the tractor.

Two AEVUZ-50/15-P-A type pneumatic actuators with the following parameters listed in Table 4 were used to control the two brake pads.

Table 4. Parameters of the selected pneumatic actuators of brake blocks

Parameter	Value	Unit
Piston diameter – D	50	[mm]
Piston rod diameter – d	16	[mm]
Cylinder stroke – s	15	[mm]
Max. allowed pressure – p_d	10	[bar]
Spring force – P_s	40	[N]
Force at 6 bar – P_m	1178	[N]

The pressure of the brake block against the rail wheel is applied by means of a lifting system and by the pneumatic supply of the actuator (from the piston rod side). The block is moved away from the wheel by the action of a spring mounted on the piston side in the actuator. When connecting the actuators directly to the compressor, the supplied pressure becomes p = 10 bar, when connected to air tanks, the supplied pressure becomes p = 8 bar.

The cross-section area A_t of the bearing surface on the piston rod side is:

$$A_t = \frac{\Pi \cdot (D^2 - d^2)}{4} = \frac{\Pi \cdot (50^2 - 16^2)}{4} = 1761.5 \text{ mm} \quad (27)$$

Hence the force on the piston rod P_r becomes:

$$P_r = p \cdot A_t - P_s \text{ [N]} \quad (28)$$

– for p = 10 bar:

$$P_r = 1 \cdot 1761.5 - 40 = 1721.5 \text{ N} \quad (29)$$

– for p = 8 bar:

$$P_r = 0.8 \cdot 1761.5 - 40 = 1369.2 \text{ N} \quad (30)$$

The gear ratio of the levers pressing the brake pad to the wheel according to the dimensions given in Fig. 5 is:

$$i_d = \frac{103 \text{ mm}}{49 \text{ mm}} = 2.1 \quad (31)$$

Hence, the force pressing the block against the surface of the wheel is:

$$P_k = \frac{P_r}{i_d} \quad (32)$$

– for p = 10 bar:

$$P_k = \frac{1721.5}{2.1} = 820 \text{ N} \tag{33}$$

– for p = 8 bar:

$$P_k = \frac{1369.2}{2.1} = 652 \text{ N} \tag{34}$$

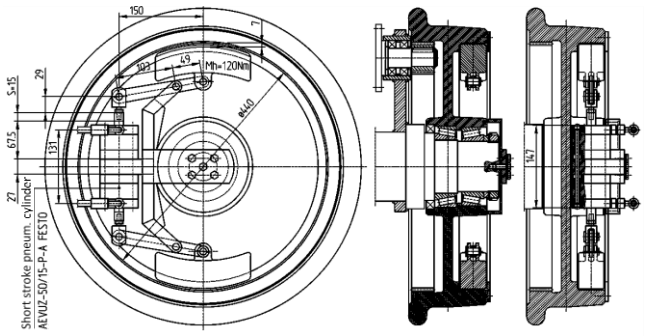

Fig. 5. Air operated friction brake

The braking torque M_h was determined for the friction conditions defined as: a cast iron block on a cast steel wheel, taking into account surface contamination, so with a sliding friction coefficient of μ = 0.65 and the friction diameter (inner surface of the wheel) D_t = 0.44 m.

$$M_h = P_k \cdot \mu \cdot \frac{D_t}{2} \tag{35}$$

– for p = 10 bar:

$$M_h = 820 \cdot 0.65 \cdot \frac{0.44}{2} \approx 120 \text{ Nm} \tag{36}$$

– for p = 8 bar:

$$M_h = 625 \cdot 0.65 \cdot \frac{0.44}{2} \approx 90 \text{ Nm} \tag{37}$$

Standard parking braking torque values in systems with hydraulic and electric motors performed using mechanical parking brakes are M_h = 120 Nm.

Conclusion

This article presents the initial concept of a road-rail vehicle. Due to the increasingly restrictive norms regarding the exhaust emission of harmful substances, it became common to seek environmentally friendly solutions that still allow for maintaining the required operating and technical parameters. The authors presented a construction design that allows for, among others, emission-free driving indoors with the use of an electric drive system. In addition, the vehicle, compared to a shunting locomotive fulfilling the same functions, was characterized by a lower purchase cost, which is expected to make such a product more attractive to potential customers.

The article includes a multi-variant analysis of the drive system selection, which took into account the selection of appropriate dimensions of the electric motor, as well as the technical parameters of the drive, gear ratio and clutch. Calculations were also done for the bearings of the guide rollers and the pneumatic brake system.

Road-rail vehicles combine the advantages of rail and road vehicles. Equipped with a diesel-electric drive system, they have additional features that are a significant advantage in the competitive market.

Nomenclature

a	acceleration [m/s^2]
BLDC	brush less direct-current motor
C	load capacity [N]
$C_{calc.}$	calculated dynamic load capacity [N]
D_k	guide roller wheel diameter [m]
F	force [N]
i	gear ratio [–]
i_c	total gear ratio [–]
k_{go}	maximum stress [MPa]
M	torque [Nm]
n	rotational speed [rpm]
N_S	power demand [kW]
p	pressure [bar]
P_z	equivalent force [N]
R_m	ultimate tensile strength [MPa]
s	stroke [mm]
V	velocity [m/s]
z	number of teeth [–]
λ	gear width factor [–]

Bibliography

[1] ANDRZEJEWSKI, M., FUĆ, P., GALLAS, D. Impact of driving style on the exhaust emission of a diesel multiple unit. *Computers in Railways XVII: Railway Engineering Design and Operation*. 2020, **199**, 365. https://doi.org/10.2495/CR200341

[2] APICELLA, B., MANCARUSO, E., RUSSO, C. et al. Effect of after-treatment systems on particulate matter emissions in diesel engine exhaust. *Experimental Thermal and Fluid Science*. 2020, **116**, 110107. https://doi.org/10.1016/j.expthermflusci.2020.110107

[3] BORZA, P.N., MACHEDON-PISU, M., CARP, M.C. Hybrid electrical storage solutions for developing reliable transport systems. *14th International Renewable Energy Storage Conference 2020 (IRES 2020)*. Atlantis Press 2021, 206-212. https://doi.org/10.2991/ahe.k.210202.030

[4] BRYK, K., ŁUKASZEWSKI, K., MEDWID, M. Symulacyjne badania bezpieczeństwa ruchu ciągnika szynowo-drogowego Claas Arion 620. *Prace Naukowe Politechniki Warszawskiej. Transport*. 2017, **116**, 21-30.

[5] CHEN, A., HUANG, T., CHEN, S. et al. Research status of electric tractor in China. *International Core Journal of Engineering*. 2019, **5**(12)**,** 99-104.

[6] CHEN, Y., XIE, B., DU, Y. et al. Powertrain parameter matching and optimal design of dual-motor driven electric

tractor. *International Journal of Agricultural and Biological Engineering*. 2019, **12**(1), 33-41. https://doi.org/10.25165/IJABE.V12I1.3720
[7] CICHY, R., CZERWIŃSKI, J. Projektowanie pojazdów dwudrogowych–wymagania prawne. *Zeszyty Naukowo-Techniczne Stowarzyszenia Inżynierów i Techników Komunikacji w Krakowie. Seria: Materiały Konferencyjne*. 2019.
[8] CRISTEA, M., MATACHE, M.G., SORICA, C.M. et al. Study on the behavior of a battery mounted on an electric tractor prototype. *INMATEH-Agricultural Engineering*. 2020, **62**(3). https://doi.org/10.35633/inmateh-62-02
[9] DAGGOLU, P.R., GOGIA, D.K., SIDDIQUIE, T.A. Exhaust after treatment system for diesel locomotive engines – a review. *Locomotives and Rail Road Transportation*. 2017, 155-168, Springer. https://doi.org/10.1007/978-981-10-3788-7_8
[10] DALLMANN, T., MENON, A. Technology pathways for diesel engines used in non-road vehicles and equipment. *International Council on Clean Transportation (ICCT)*: Washington 2016.
[11] DASZKIEWICZ, P., KURC, B., PIGŁOWSKA, M. et al. Fuel cells based on natural polysaccharides for rail vehicle application. *Energies*. 2021, **14**(4), 1144. https://doi.org/10.3390/en14041144
[12] DASZKIEWICZ, P., MERKISZ, J., MEDWID, M. et al. Assessment of toxic compounds emission of rail-road tractor during works on tracks. *Pojazdy Szynowe*. 2018, **4**, 1-8. https://doi.org/10.53502/RAIL-138518
[13] DING, Z., LI, B. Design and analysis of the suspension for electric tractor. *IOP Conference Series: Materials Science and Engineering*. IOP Publishing. 2019. 012077. https://doi.org/10.1088/1757-899X/493/1/012077
[14] ENRICI, P., BOUBAKER, N., MATT, D. Bar winding for the low-voltage motorization of an electric tractor. *2020 International Conference on Electrical Machines (ICEM)*. IEEE. 2020. 1711-1717. https://doi.org/10.1109/ICEM49940.2020.9270906
[15] FAG Bearings Catalog.
[16] GALLAS, D., MERKISZ, J., DASZKIEWICZ, P. Investigation of exhaust emissions from a shunting locomotive and a rail diagnostics machine. *SAE Technical Paper* 2020-01-2216. 2020. https://doi.org/10.4271/2020-01-2216
[17] GAO, H., XUE, J. Modeling and economic assessment of electric transformation of agricultural tractors fueled with diesel. *Sustainable Energy Technologies and Assessments*. 2020, **39**, 100697. https://doi.org/10.1016/j.seta.2020.100697
[18] GORYCA, Z. Metody sterowania silników BLDC. *Prace Naukowe Instytutu Maszyn, Napędów i Pomiarów Elektrycznych Politechniki Wrocławskiej*. 2012, **66**, 32-47.
[19] KIM, W.S., BAEK, S.Y., KIM, T.J. et al. Work load analysis for determination of the reduction gear ratio for a 78 kW all wheel drive electric tractor design. *Korean Journal of Agricultural Science*. 2019, **46**(3), 613-627. https://doi.org/10.7744/kjoas.20190047
[20] LI, T., XIE, B., WANG, R. Design and experiments of electronic steer-by-wire system in electric tractor. *IOP Conference Series: Earth and Environmental Science*. IOP Publishing. 2019, 032108. https://doi.org/10.1088/1755-1315/252/3/032108
[21] LI, Y., HALLERMAN, E.M., WUET, K. et al. Insect-resistant genetically engineered crops in China: development, application, and prospects for use. *Annual review of entomology*. 2020, **65**, 273-292. https://doi.org/10.1146/annurev-ento-011019-025039
[22] LIU, H., CHEN, G., XIE, C. et al. Research on energy-saving characteristics of battery-powered electric-hydrostatic hydraulic hybrid rail vehicles. *Energy*. 2020, **205**, 118079. https://doi.org/10.1016/j.energy.2020.118079
[23] LIU, J., XIA, C., JIANG, D. et al. Development and testing of the power transmission system of a crawler electric tractor for greenhouses. *Applied Engineering in Agriculture*. 2020, **36**(5), 797-805. https://doi.org/10.13031/aea.13360
[24] LIU, M., WEI, C., XU, L. Development of cooperative controller for dual-motor independent drive electric tractor. *Mathematical Problems in Engineering*. 2020. https://doi.org/10.1155/2020/4826904
[25] LU, M., ZHANG, Y., WU, Y. et al. Optimization of MTPA algorithm of permanent magnet synchronous motor for electric tractor. *2018 21st International Conference on Electrical Machines and Systems (ICEMS)*. IEEE. 2018, 371-375. https://doi.org/10.23919/ICEMS.2018.8549212
[26] LU, Z.X., HOU, X., DENG, X. Matching design and traction tests for driving system of series hybrid electric tractor. *Journal of Nanjing Agricultural University*. 2017, **40**(5), 928-935.
[27] MEDWID, M. Hybrydowe pojazdy kolejowo-drogowe zaprojektowane i wytwarzane w Polsce. *TTS Technika Transportu Szynowego*. 2005, **11**, 45-53.
[28] MEDWID, M., DASZKIEWICZ, P., CZERWIŃSKI, J. et al. Rail-road tractor with diesel-electric drive. *Pojazdy Szynowe*. 2019, **3**, 15-23. https://doi.org/10.53502/RAIL-138536
[29] MEDWID, M., STAWECKI, W., CZERWIŃSKI, J. et al. Structure modeling of the CLAAS ARION 620 road-rail shunting tractor. *Pojazdy Szynowe*. 2017, **2**, 1-14. https://doi.org/10.53502/RAIL-138451
[30] MEDWID, M., STAWECKI, W., CZERWIŃSKI, J. et al. Multi-purpose rail-road tractor of the new generation. *Pojazdy Szynowe*. 2016, **3**, 1-12. https://doi.org/10.53502/RAIL-138736
[31] MEDWID, M., JAKUSZKO, W., KAZIMIERCZAK, E. Structural features of the tractor selected for adaptation to the new road-rail vehicle. *Pojazdy Szynowe*. 2017, **3**, 1-11. https://doi.org/10.53502/RAIL-138445
[32] MEDWID, M., BRYK, K., WITKOWSKI, D. et al. Strength simulation tests of the load-bearing structure in a rail-road CLAAS ARION 610 tractor. Part 1. *Pojazdy Szynowe*. 2020, **2**, 1-11. https://doi.org/10.53502/RAIL-138546
[33] MELO, R.R., ANTUNES, F.L., DAHER, S. et al. Conception of an electric propulsion system for a 9 kW electric tractor suitable for family farming. *IET Electric Power Applications*. 2019, **13**(12), 1993-2004. https://doi.org/10.1049/IET-EPA.2019.0353
[34] MERKISZ, J., RYMANIAK, Ł., LIJEWSKI, P. et al. Tests of ecological indicators of two-way vehicles meeting Stage IIIB and Stage IV standards in real operating conditions. *Pojazdy Szynowe*. 2020, **1**, 1-9. https://doi.org/10.53502/RAIL-138495
[35] MICHALAK, P., MERKISZ, J., STAWECKI, W. et al. The selection of the engine unit-main engine generator during the modernization of the 19D/TEM2 locomotive. *Combustion Engines*. 2020, **182**(3)**,** 38-46. https://doi.org/10.19206/CE-2020-307
[36] MOCERA, F. A model-based design approach for a parallel hybrid electric tractor energy management strategy using hardware in the loop technique. *Vehicles.* 2021, **3**(1), 1-19. https://doi.org/10.3390/vehicles3010001
[37] MOCERA, F., SOMÀ, A. Analysis of a parallel hybrid electric tractor for agricultural applications. *Energies*. 2020, **13**(12), 3055. https://doi.org/10.3390/en13123055
[38] NGUYEN, T., PHAM, M.H., LE ANH, T. Spray, combustion, performance and emission characteristics of a common

rail diesel engine fueled by fish-oil biodiesel blends. *Fuel*. 2020, **269**, 117108. https://doi.org/10.1016/j.fuel.2020.117108

[39] OLABI, A.G., MAIZAK, D., WILBERFORCE, T. Review of the regulations and techniques to eliminate toxic emissions from diesel engine cars. *Science of The Total Environment*. 2020, **748,** 141249. https://doi.org/10.1016/j.scitotenv.2020.141249

[40] ÖZDEMIR, M.R., YANGAZ, M.U., YILMAZ, I.T. Energy, exergy and exergo-economic characteristics of hydrogen enriched hydrocarbon-based fuels in a premixed burner. *Energy Sources, Part A: Recovery, Utilization, and Environmental Effects*. 2021, 1-18. https://doi.org/10.1080/15567036.2021.1895371

[41] RYMANIAK, Ł., KAMIŃSKA, M., SZYMLET, N. et al. Analysis of harmful exhaust gas concentrations in cloud behind a vehicle with a spark ignition engine. *Energies*. 2021, **14**(6)**,** 1769. https://doi.org/10.3390/en14061769

[42] RYMANIAK, Ł., LIJEWSKI, P., KAMIŃSKA, M. et al. The role of real power output from farm tractor engines in determining their environmental performance in actual operating conditions. *Computers and Electronics in Agriculture*. 2020, **173**, 105405. https://doi.org/10.1016/j.compag.2020.105405

[43] SHANG, G., ZHANG, J., ZHANG, J. Research on control strategy of tracked electric tractor drive system. *Journal of Chongqing University of Technology (Natural Science)*. 2017, **33**(11)**,** 32-38.

[44] SPENCER, J. Electric tractor powered by a cable. *Farmer's Weekly*, 2019, 19013, 52.

[45] TARASCON, J-M. Na-ion versus Li-ion batteries: Complementarity rather than competitiveness. *Joule*. 2020, **4**(8), 1616-1620. http://doi.org/10.1016/j.joule.2020.06.003

[46] TOMASZEWSKI, S., DASZKIEWICZ, P., ANDRZEJEWSKI, M. et al. Economic and ecological analysis of vehicles used in railways. *Transport Economics and Logistics*. 2020, **81**, 57-69. https://doi.org/10.26881/etil.2019.81.05

[47] TSENG, K-C., CHANG, Y-C, CHENG, C-A. Implementation and analysis of ultracapacitor charger in hybrid energy-storage system for electric-vehicle applications. *IET Power Electronics*. 2020, **13**(9), 1858-1864. https://doi.org/10.1049/iet-pel.2019.1469

[48] URBAN, M. Modern hybrid propulsion systems for rail and marine applications: environmental and customer benefits through optimized system integration of proven diesel technology with latest electrical innovation. *Heavy-Duty-, On- und Off-Highway-Motoren 2019*. Springer Vieweg, Wiesbaden 2020, 185-196. https://doi.org/10.1007/978-3-658-31371-5_14

[49] VOGT, H.H., ALBIERO, D., SCHMUELLING, B. Electric tractor propelled by renewable energy for small-scale family farming. *2018 Thirteenth International Conference on Ecological Vehicles and Renewable Energies (EVER)*. IEEE, 2018. 1-4. https://doi.org/10.1109/EVER.2018.8362344

[50] WU, Z., XIE, B., LI, Z. et al. Modelling and verification of driving torque management for electric tractor: Dual-mode driving intention interpretation with torque demand restriction. *Biosystems Engineering*. 2019, **182**, 65-83. https://doi.org/10.1016/j.biosystemseng.2019.04.002

[51] ZHANG, X. Design theory and performance analysis of electric tractor drive system. *International Journal of Engineering Research & Technology (IJERT)*. 2017, 2278-0181.

[52] ZHANG, Z., YE, J., TAN, D. et al. The effects of Fe_2O_3 based DOC and SCR catalyst on the combustion and emission characteristics of a diesel engine fueled with biodiesel. *Fuel*. 2021, **290**, 120039. https://doi.org/10.1016/j.fuel.2020.120039

[53] ZIÓŁKOWSKI, A., FUĆ, P., LIJEWSKI, P. et al. Analysis of exhaust emission measurements in rural conditions from heavy-duty vehicle. *Combustion Engines*, 2020, **182**(3), 54-58. https://doi.org/10.19206/CE-2020-309

Paweł Daszkiewicz, DEng. – Łukasiewicz Research Network – Rail Vehicle Institute "TABOR", Poland.
e-mail: *p.daszkiewicz@tabor.com.pl*

Maciej Andrzejewski, DEng. – Łukasiewicz Research Network – Rail Vehicle Institute "TABOR", Poland.
e-mail:
maciej.andrzejewski@tabor.lukasiewicz.gov.pl

Prof. Marian Medwid, DSc., DEng. – Łukasiewicz Research Network – Rail Vehicle Institute "TABOR", Poland.
e-mail: *marian.medwid@tabor.lukasiewicz.gov.pl*

Patryk Urbański, MEng. – Łukasiewicz Research Network – Rail Vehicle Institute "TABOR", Poland.
e-mail: *patryk.urbanski@tabor.com.pl*

Maksymilian Cierniewski, MEng. – Łukasiewicz Research Network – Rail Vehicle Institute "TABOR", Poland.
e-mail:
maksymilan.cierniewski@tabor.lukasiewicz.gov.pl

Aleksandra Woch, MEng. – Łukasiewicz Research Network – Rail Vehicle Institute "TABOR", Poland.
e-mail: *aleksandra.woch@tabor.lukasiewicz.gov.pl*

Natalia Stefańska, MEng. – Łukasiewicz Research Network – Rail Vehicle Institute "TABOR", Poland.
e-mail: *natalia.stefanska@tabor.lukasiewicz.gov.pl*